IEEE Access
Multidisciplinary | Rapid Review | Open Access Journal

Received April 20, 2019, accepted May 7, 2019, date of publication May 17, 2019, date of current version October 22, 2019.

Digital Object Identifier 10.1109/ACCESS.2019.2917619

Design of Automatic Carrier-Landing Controller Based on Compensating States and Dynamic Inversion

LIPENG WANG[1], ZHI ZHANG[1], QIDAN ZHU[1], AND ZIXIA WEN[2]
[1]College of Automation, Harbin Engineering University, Harbin 150001, China
[2]AVIC Xi'an Flight Automatic Control Research Institute, Xi'an 710065, China

Corresponding author: Zhi Zhang (zz_heu@163.com)

This work was supported in part by the National Natural Science Foundation of China under Grant 61803116 and Grant 61603110, and in part by the Fundamental Research Funds for the Central Universities of China under Grant 3072019CFJ0405.

ABSTRACT In this paper, a design scheme of automatic carrier landing system (ACLS) control law based on compensating states and dynamic inversion is proposed, in order to eliminate landing risk and air wake disturbance and improve flight quality during landing. First of all, the mathematical model for an aircraft during carrier landing is established and transformed into a low-order linear perturbed model with the involved state variables, which denotes the reference model. Second, a high-dimension field of the landing risk is addressed, which reflects the current and the potential risk degrees due to the subjective prediction of the pilots. The coefficients of the landing risk field are established based on a pilot behavioral model. Third, a concept of compensating states is proposed by this paper. On one hand, the compensating states of the air wake disturbance are estimated from the nonlinear and reference models. On the other hand, the compensating states of the landing risk are composed of the high-dimension risk field. Fourth, automatic carrier landing control law is built with the compensating states of air wake and landing risk, nonlinear dynamic inversion, and feedback signals of the flight states. In the rolling optimization progress, the landing risk, air wake, and nonlinear factors of flight states are dynamically introduced to control the state deviations and suppress landing risk. Test results based on a semi-physical simulation platform indicate that the proposed algorithm brings about an excellent landing performance and an ability to eliminate landing risk and air wake.

INDEX TERMS Automatic carrier landing system, nonlinear dynamic inverse, compensating states, landing risk, air wake.

I. INTRODUCTION

The terminal carrier approach of a carrier-based aircraft is filled with risks and dangers, which are induced by the disturbance of air wake, carrier movement, and any other hardly predicted influential factors. Especially, the air wake seriously affects the safety of aircraft landing. Air wake is a kind of moving airflow across the carrier, composed of free-air turbulence, the steady component, the periodic component, and random component. By now, the recovery of an aircraft aboard a carrier is mainly completed by human pilots. However, artificial landing, i.e., carrier landing completed by manual control, is still a difficult task for most excellent pilots, because it is heavily influenced by visibility, deck swing, psychological fluctuations, mental stress, and so on. More than 70% of fatal aviation accidents are due to the poor judgment of pilots [1]. Between 2011 and 2012, there are 11 Class-A mishaps in U.S. Navy due to incorrect decision and controls of the human pilots [2]. Especially in difficult sea conditions, the destructive collision accidents are easily caused by abnormal controls of pilots [3]. In 1960s, ACLS provided the capability for U.S. Navy automatic hands-off landing [4], and it is improved for some times [5]. Compared with the artificial landing, automatic landing not only reduce the stress of human pilots from the complex manipulating circumstance, but also maintain high precision in the rough sea condition. Therefore, the automatic landing technology is the development trend for the carrier-based aircrafts.

Control algorithm is the core technology in ACLS, which is designed through different methods by the scholars.

The associate editor coordinating the review of this manuscript and approving it for publication was Xudong Zhao.

Urnes and Hess [5] adopt a classic ACLS control method, in which the inner, middle, and outer loops of a typical ACLS structure is addressed based on a proportion integration differentiation (PID) method. It is worth mentioning that the sink rate and normal acceleration are reacted on main loop of ACLS. The robust characteristics and performances are analyzed in the time- and frequency-domains in detail. PID method is widely utilized to develop ACLS control law, such as in [6] and [7]. Especially, the structures and control patterns in [5]–[7] inspire the present paper. With the development of other control methods, scholars are attempting to construct new structure for ACLS control laws. Lungu and Lungu [8], [9] introduce H$-\infty$ and dynamic inversion to reduce crosswind disturbance and sensor errors. The reference model of aircraft landing and safety envelope in this literature are rarely researched by other references. Neural network (NN) manifests excellent performance in dealing with nonlinear model. Reference [10] integrated NN and PID to construct control law in the control law for glide slope and flare. Regrettably, the method is suitable for land-based aircraft, lacking the consideration of the deck motion, air wake disturbance, and other special conditions. Reference [11] establishes a guidance law of the lateral landing by NN, which controls the aircraft to automatically lineup with the trajectory. The sliding mode control is also a popular method to solve nonlinear problem. The sliding mode control with a fuzzy controller is integrated to design an ACLS control law, which is superior to the conventional PID method [12]. Likewise, Reference [13]–[15] adopted backstepping technology with other intelligent control methods to reject uncertainty of the landing model. Zhen *et al.* proposed a preview control to establish an autolanding controller in longitudinal and lateral directions [16]. Wang *et al*. adopted a trajectory tracking method based on robust fuzzy theory and adaptive neural control [17], [18], in which the stability analysis of the closed-loop system inspires the present paper. Some researchers adopt model predictive control (MPC) [19], quantitative feedback theory [20], brain storm optimization [21], and pigeon$-$ inspired optimization [22]. However, the aforementioned methods only focus on the special problems, such as control precision and uncertainties of landing model, which indicates that they lack the abilities of solving the general problems.

By contrast, the nonlinear dynamic inversion (NDI) method is not only an excellent option to solve the general problems, but also easy to be improved with the auxiliary strategies. In some previous research works, the NDI method has been used to design the nonlinear ACLS control law. Lungu et al. utilizes NDI and H$-\infty$ to establish a lateral automatic landing system [23], which is skilled in eliminating sensor errors and wind disturbance. Reference [24] proposes an incremental NDI method with a Kalman filter to predict the wind turbulence. Reference [25] establishes an innovative motion model for the aircraft based on NDI, which could reduce different kinds of wind turbulence. Reference [26] designs an automatic landing control law for the impaired aircraft based on feedback linearization. However, the most affecting parameter, such as the wind disturbance, is not considered. Reference [27] integrates fuzzy-logic and dynamic inversion to reduce the crosswind during landing. Particularly, some local stability and control characteristics are analyzed in detail. Zhao et al. introduced the nonlinear control methods based on adaptive backstepping technique and fuzzy hierarchical sliding-mode control in detail [28], [29]. The adaptive control thought in these references enlightens this paper. Reference [30] proposes a nonlinear generalized dynamic inversion to construct a model of tracking desired trajectory, and the analysis of algorithm stability is rigorously presented. However, there are some disadvantages to establish ACLS control law on basis of the traditional NDI. First, the coupling between longitudinal direction and lateral direction is seldom researched in the previous literature. Second, the control methods proposed by the previous scholars hardly consider the air wake and different landing risk conditions.

Landing risk is one of the most important safety issues about the landing process. Many scholars analyze and establish the landing risk model in different viewpoints. Luxhoj [31] proposes a probability model of landing risk for the unmanned aircraft system (UAS) based on Bayesian network. Identification of risk parameters and correlation analysis of risk factors are characteristic in this literature. Tian and Lungu [32] developed a landing risk comprising mishap probability, time margin, and mishap severity. Reference [33] concludes the previous research achievement about UAS landing risk, and analyzes the similarity and differences of 33 landing risk models. Reference [34] concludes 21 factors affecting landing risk from 293 quick access recorders, and establishes a regression model of operations and landing performance based on flight parameter characteristics of landing risk. Other risk models include Pareto distribution [35], system-theoretic process analysis [36], risk probability theory [37], and so on. It is noted that the satisfaction index of the pilots is one of the most important evaluation indices in the U.S. military standard, but the previous landing risk models seldom consider the feeling and perception of the pilots. In another aspect, the previous risk model is hardly introduced into the automatic landing system. Some scholars specially research the method to estimate the wind velocities. A Kalman filter theory is utilized to estimate wind speed components [38]. It is a pity that the instantaneous components of air wake cannot be acquired by this way, so this method does not fit for designing the disturbance estimator for ACLS. However, the thought of reference data inspires the present paper to establish a reference model. A novel moving horizon controller is designed to estimate wind velocities [39]. However, the estimate of lateral wind velocity is limited, and the nonlinear problem in real time is not considered. The discrete sampling form is utilized by the present paper to deal with the continuous signals.

The whole landing process is full of complex influences. However, the traditional ACLS control law usually reduces the air wake disturbance and deals with landing nonlinearity

based on the stability of control system. In addition, the landing risk is seldom considered in the design of ACLS control law. Therefore, it is valuable to design an innovative ACLS control law, specially dealing with disturbances, nonlinearity, and landing risk. This paper proposes an innovative NDI method, which considers the landing risk and the air wake disturbance, and guarantees the high performance. According to Reference [5], the step of autopilot in F/A-18 is 50 ms, and the simulated step in this paper is adopted 20 ms. The algorithm proposed by this paper can eliminate the landing risk and disturbance in real time. The structure of this paper is shown by Fig. 1. The landing model of F/A-18 aircraft integrated with the longitudinal and lateral directions is established on the basis of numerical software, which is the model foundation of this paper. An air wake estimator based on the reference model is built to predict the air wake states. A high-dimension field of the landing risk is brought forward based on pilots' experiences. The compensating states of the air wake and landing risk are designed, which are introduced to the NDI control structure to establish ACLS control law.

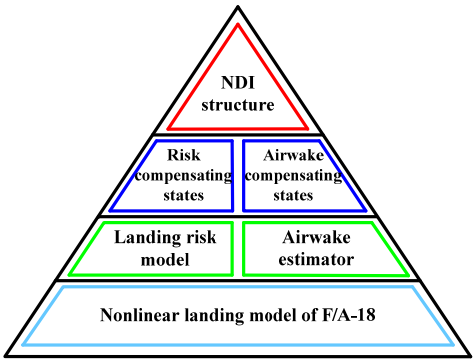

FIGURE 1. Structure of the present paper.

The rest of this paper is organized as follows. In section 2, a nonlinear landing model of the F/A-18 aircraft in the longitudinal and lateral directions is established. Furthermore, a linear reference model is also built based on the equilibrium states. In section 3, an estimator of air wake during landing is designed based on the reference model. A high-dimension field of landing risk is developed in section 4. The control principle and structure of a novel NDI with the compensating states is described in section 5. Some simulations on a semi-physical platform are presented in section 6. Section 7 concludes the whole paper.

II. LANDING MODEL OF CARRIER-BASED AIRCRAFT

Reference [40], [41] describe the nonlinear landing model and the flight test data of F/A-18 Hornet aircraft in the longitudinal and lateral directions, which provide some very valuable information, including the form of nonlinear landing functions, aerodynamic parameter, and control surface and actuator configurations of F/A-18. Parameters of F/A-18 in this paper are referred to Reference [40], [41]. As the same landing model of Reference [41] is utilized here, this paper adopts the same presentation for the motion equations of F/A-18 as Reference [41]. A six degree of freedom 9-state mathematical model for the F/A-18 aircraft is presented by the following:

$$\begin{cases} \dot{V} = -\dfrac{1}{m}(D\cos\beta - Y\sin\beta) + g(\cos\phi\cos\theta\sin\alpha\cos\beta \\ \qquad + \sin\phi\cos\theta\sin\beta - \sin\theta\cos\alpha\cos\beta) \\ \qquad + \dfrac{T}{m}\cos\alpha\cos\beta \\ \dot{\alpha} = -\dfrac{1}{mV\cos\beta}L + q - \tan\beta(p\cos\alpha + r\sin\alpha) \\ \qquad + \dfrac{g}{V\cos\beta}(\cos\phi\cos\theta\cos\alpha + \sin\alpha\sin\theta) \\ \qquad - \dfrac{T\sin\alpha}{mV\cos\beta} \\ \dot{\beta} = \dfrac{1}{mV}(Y\cos\beta + D\sin\beta) + p\sin\alpha - r\cos\alpha \\ \qquad + \dfrac{g}{V}\cos\beta\sin\phi\cos\theta + \dfrac{\sin\beta}{V}(g\cos\alpha\sin\theta \\ \qquad - g\sin\alpha\cos\phi\cos\theta + \dfrac{T}{m}\cos\alpha) \end{cases} \tag{1}$$

$$\begin{bmatrix} \dot{p} \\ \dot{q} \\ \dot{r} \end{bmatrix} = \begin{bmatrix} I_{zz}/k & 0 & I_{xz}/k \\ 0 & 1/I_{yy} & 0 \\ I_{xz}/k & 0 & I_{xx}/k \end{bmatrix} \left(\begin{bmatrix} l \\ m \\ n \end{bmatrix} - \begin{bmatrix} 0 & -r & q \\ r & 0 & -p \\ -q & p & 0 \end{bmatrix} \begin{bmatrix} I_{xx} & 0 & -I_{xz} \\ 0 & I_{yy} & 0 \\ -I_{xz} & 0 & I_{zz} \end{bmatrix} \begin{bmatrix} p \\ q \\ r \end{bmatrix} \right) \tag{2}$$

$$\begin{bmatrix} \dot{\phi} \\ \dot{\theta} \\ \dot{\psi} \end{bmatrix} = \begin{bmatrix} 1 & \sin\phi\tan\theta & \cos\phi\tan\theta \\ 0 & \cos\phi & -\sin\phi \\ 0 & \sin\phi\sec\theta & \cos\phi\sec\theta \end{bmatrix} \begin{bmatrix} p \\ q \\ r \end{bmatrix} \tag{3}$$

where, landing states in longitudinal direction are: approach velocity V, angle of attack (AOA) α, pitch angle θ, and pitch rate q. Landing states in lateral direction are: sideslip angle β, roll angle ϕ, yaw angle ψ, roll rate p, and yaw rate r. I_{xx}, I_{yy} and I_{zz} are the moment of inertia around the corresponding coordinate axis. I_{xz} is multiplication cross of product. $k = I_{xx}I_{zz} - I_{xz}^2$. T denotes thrust.

D, L and Y are the aerodynamic drag force, lift force and side force, and M_r, M_t and M_n are roll moment, pitch moment and yaw moment, which can be shown below:

$$\begin{cases} D = \bar{q}SC_D(\alpha, \beta, \delta_s) \\ L = \bar{q}SC_L(\alpha, \beta, \delta_s) \\ Y = \bar{q}SC_Y(\alpha, \beta, \delta_a, \delta_r) \\ M_r = \bar{q}SbC_L(\alpha, \beta, \delta_a, \delta_r, p, r, V) \\ M_t = \bar{q}SC_L(\alpha, \delta_s, q, V) \\ M_n = \bar{q}SbC_n(\alpha, \beta, \delta_a, \delta_r, p, r, V) \end{cases} \tag{4}$$

where, δ_s, δ_a and δ_r are the deflection angle of stabilator, rudder and aileron, respectively. In this paper, it is noted that the aileron and stabilator are the direct actuators in the lateral and longitudinal loops, respectively. In other words, the positions on the lateral and longitudinal planes are controlled by the aileron and stabilator, respectively. The rudder is introduced

into the lateral loop, but it does not directly control the lateral position.

The air wake is an important effect factor for the aircraft landing. The air wake component is not included in Eqs. (1)-(3), and the air wake cannot be directly measured due to randomness. Furthermore, the aircraft may descend caused by the air wake during landing, and this situation is very dangerous nearby the carrier stern. To this end, this paper adopts a reference model to estimate the air wake, which provides the air wake states for ACLS. The reference model is established according to the following two principles:

(1) The reference model is a low-order and linear model to guarantee the computation speed, and the output of the reference model does not lag behind the output of nonlinear landing model.
(2) The reference model must sufficiently reflect the accurate disturbance of the air wake.

Therefore, this paper establishes a linear landing model based on the equilibrium states, which is treated as the reference model of F/A-18 aircraft. The equilibrium states are the following [42]: $V_t = 69.9$ m/s, $\alpha_t = 8.3$ deg, $\theta_t = 4.9$ deg, $q_t = 0$ deg/s, $\beta_t = 0$ deg, $\phi_t = 0$ deg/s, $\psi_t = 0$ deg/s, $p_t = 0$ deg/s, $r_t = 0$ deg/s. The subscript t represents the landing states are equilibrium ones. Through the trim function in Matlab tools, the linear landing model of the aircraft can be represented as follows:

$$\begin{cases} \dot{x} = Ax + Bu \\ y = Cx + Du \end{cases} \tag{5}$$

where, A, B, C and D are the system matrices, which are not described here due to the space limitation.

The equation above is a linear and low-order description. The order of reference model is less than that of the nonlinear landing model, thus it calculates the reference signals quickly and does not delay the simulation time. The reference model is evaluated near the equilibrium states, and could represent the landing characteristics. The model of Eq. (5) will be introduced to estimate the immeasurable air wake disturbance. It is assumed by this paper that the landing states in Eqs. (1)-(3) can be observed and measured, which are directly utilized in the structure of NDI controller.

III. AIR WAKE ESTIMATOR BASED ON REFERENCE MODEL

The air wake is inevitable during the carrier-based aircraft landing. Great measures have been taken to eliminate the influences of air wake in the previous literatures. This paper will design an air wake estimator to calculate the velocity components of air wake, which are introduced into the ACLS control loops and increase the robust characteristic of ACLS [43], [44]. As the reference model is the linearized model of nonlinear landing model under the condition of equilibrium states, the air wake estimator is based on the nonlinear landing model and the reference model. It is note that the principle of estimating in this paper is suitable under the condition of equilibrium states.

The approach velocity components V_{xg}, $V_{yg}$and V_{zg}in ground coordinate system could be represented below:

$$\begin{bmatrix} V_{xg} \\ V_{yg} \\ V_{zg} \end{bmatrix} = T_{gb}T_{ba} \begin{bmatrix} V \\ 0 \\ 0 \end{bmatrix} \tag{6}$$

where, T_{gb} and T_{ba} are respective transformation matrices from body coordinate system to ground coordinate system, and wind coordinate system to body coordinate system.

The principle of estimating air wake disturbance is shown by Fig. 2. In order to conveniently simulate in the subsequent sections and illustrate the principle of air wake estimator, this paper adopts the discrete-time states and updates states of the nonlinear and linear landing model every 20 ms. The time index is represented by k.

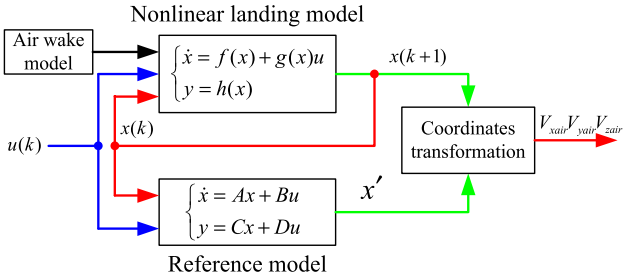

FIGURE 2. The principle of estimating air wake disturbance.

The inputs of the nonlinear and linear landing model include the landing states $x(k)$ from the previous outputs of nonlinear model and the current action of the actuators $u(k)$. What's more, the air wake components from an air wake module [45] are put into the nonlinear model, and these disturbances are unknown variables for the linear model. Therefore, under the condition of the same initial states and actuator actions, the air wake can be estimated based on the differences between the nonlinear and linear landing model outputs at step $k + 1$. It is noted that:

(1) $y = h(x)$ means the output of the nonlinear landing model in the figure below.
(2) The estimator starts from the second step, because the linear landing model needs an input from the output of the nonlinear landing model.

In ground coordinate system, the velocity components from the nonlinear landing model and the reference model are $[V_{xgr}, V_{ygr}, V_{zgr}]$ and $[V_{xgf}, V_{ygf}, V_{zgf}]$. The components of the air wake disturbanceV_{xair}, V_{yair} and V_{zair} could be described below:

$$\begin{bmatrix} V_{xair} \\ V_{yair} \\ V_{zair} \end{bmatrix} = \begin{bmatrix} V_{xgr} - V_{xgf} \\ V_{ygr} - V_{ygf} \\ V_{zgr} - V_{zgf} \end{bmatrix} \tag{7}$$

The equation above estimates the air wake disturbance, which will be introduced into NDI control structure as one of the compensating states.

Remark 1: The estimating principle of the air wake is proposed based on the nonlinear and linear landing models, and the air wake estimator can provide the disturbance components for the following control law algorithm.

IV. HIGH-DIMENSION FIELD OF LANDING RISK BASED ON RANDOM PROBABILITY

In many previous literatures, the deviations of the landing states are directly considered as the landing risk, which is unreasonable, and there are two disadvantages about it:

(1) The same landing states in different positions may result in different risk. For example, if there is -2 degrees pitch deviation on the higher position or lower position, the lower condition is more dangerous.

(2) The different landing states in different positions may result in same risk. For example, if there are -6 m/s and -3 m/s velocity deviations in the 1200 m and 400 m approach distances, both conditions have the same dangerous levels.

The descriptions above are so complex and nonlinear that it is hard to use a mathematic deviation to describe the landing risk. Inspired by the artificial landing process, this paper intends to establish a landing risk based on experiences of the pilots. The judgment and decision in the subjectivity of pilots could reflect the complexity of the influence factors, variability of the dynamic disturbance, and nonlinearity of the landing risk. In addition, flying quality decided by the satisfaction from the artificial pilots is an important index in ACLS control law. This paper describes the landing state risks by the probability density, as follows:

$$f(x) = \frac{1}{\sqrt{2\pi}\sigma_x} \exp(-\frac{(x-\mu_x)^2}{2\sigma_x^2}) \tag{8}$$

where, $f(x)$ is the danger level perceived by the pilots' subjectivity. μ_x and σ_x are the mean and variance of the landing state deviations. Based on many simulations through the pilot behavioral model, μ_x and σ_x of the corresponding landing states can be acquired. This paper proposes a high-dimension field of landing risk, which are constituted by the corresponding landing state risks on the different three-dimension positions. According to the description of normal distribution, this paper describes the danger levels of corresponding landing state deviations based on μ_x and σ_x of normal distribution. Since 99.74% possibilities are included in the interval $[-3\sigma, 3\sigma]$, this paper divides σ_x into 10 parts from $0.3\sigma_x$ to $3.0\sigma_x$.

The pilots' behavioral model in [3] is introduced by this paper, and 100 landing experiments are executed. It is noted that 100 different kinds of pilots based on Reference [3] are chosen in the experiments, and the levels of pilot include *Level-S* and *Level-A*, which can represent high capability of excellent pilots. However, capability indices of each pilot from *Level-S* and *Level-A* are different, which can provide better diversity of the results. The initial conditions of experiments are: the initial vertical deviation (m) is $[-20, 20]$, the initial lateral deviation (m) is $[-20, 20]$, the approach velocity (m/s) is [50], [80], the pitch angle (deg) is [3], [7], the roll angle (deg) is $[-10, 10]$, the sink rate (m/s) is [2, 6], and the drift rate (m/s) is $[-3, 3]$. It is noted that the states above are all stochastic parameters to traverse all kinds of conditions. A serial of landing state curves with approach distance can be got from the simulation. The danger levels figure of the corresponding landing state deviations are shown by different colors in the figures below.

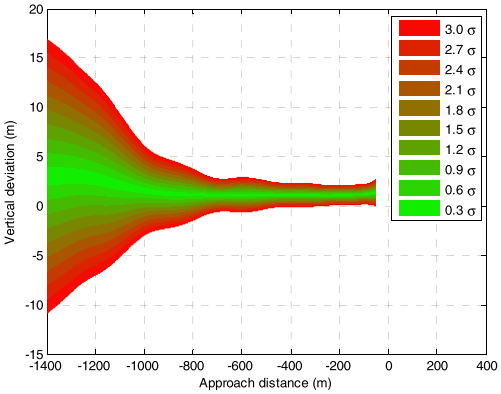

FIGURE 3. Vertical deviation danger level figure.

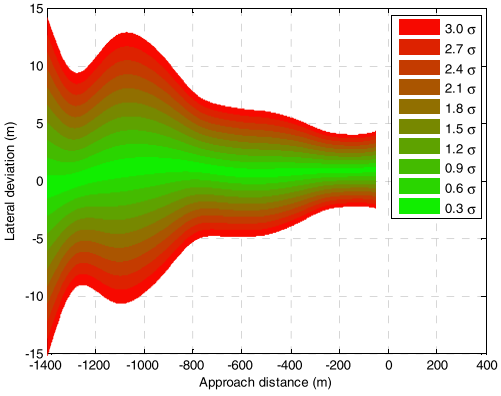

FIGURE 4. Lateral deviation danger level figure.

Noticing that there are several landing states in the longitudinal and lateral loops, each landing danger level is represented by a three-dimension figure, and all the landing danger levels construct the whole high-dimension field of landing risk. The probabilities of landing state $P(X, Y, Z)$ are described as follows

$$P(X, Y, Z) = k_{dist} \int_0^X \int_0^Y \int_0^Z f(t_x) g(t_y) h(t_z) dt_x dt_y dt_z \tag{9}$$

where, $f(t_x)$ is the probability density of lateral deviation. $g(t_y)$ is the probability density of vertical deviation. It is noted that $h(t_z)$ is the probability density of other certain one state deviation, which is one of the velocity deviation, roll angle deviation, pitch angle deviation, sink rate deviation, and drift rate deviation. The equation above proposed by this paper aims to establish some three-dimension landing

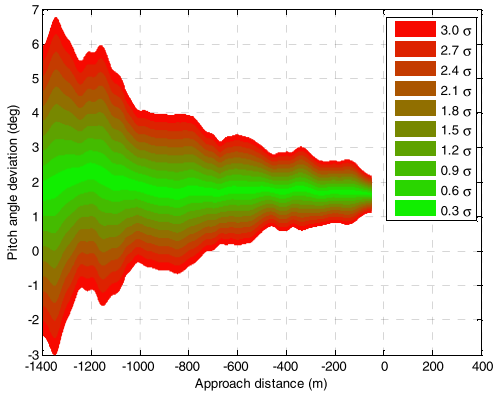

FIGURE 5. Pitch angle deviation danger level figure.

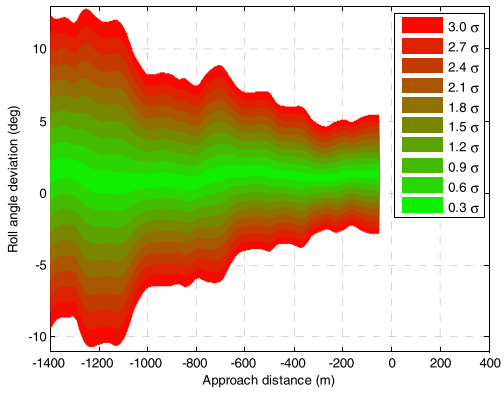

FIGURE 6. Roll angle deviation danger level figure.

risk field, which have the same x-axis (lateral deviation) and y-axis (vertical deviation), and z-axis is other certain one state deviation (roll angle deviation, or pitch angle deviation, and so on). X, Y, Z are respectively the random variable of lateral deviation, vertical deviation, and other certain one state deviation. k_{dist} is a linear coefficient of the approach distance in this paper. According to the principle of the triple integral in the calculus, Eq. (9) represents the danger probability based on the three landing state deviatons (X, Y, Z). The weighting parameter k_{dist} represents the landing risk in different distance. Therefore, the landing risk model is established by the foundation of mathematics. Based on the simulations above, a serial of three-dimension figures with approach distance, lateral deviation or vertical deviation, and other certain one state deviation are acquired. These three-dimension figures structure a quantized high-dimension field of landing risk. When approach distance is 1000 m, this paper chooses two typical landing state risks (velocity and pitch angle) to show below.

As shown by the figures above, the axes of three-dimension figures are: (1) approach distance; (2) vertical deviation or lateral deviation; (3) pitch angle deviation or velocity deviation. According to the simulation above and state deviation probabilities, this paper normalizes the danger levels, and utilizes different colors to represent the danger levels. The landing risk is belong to [0.05, 0.95]. Though the landing risk

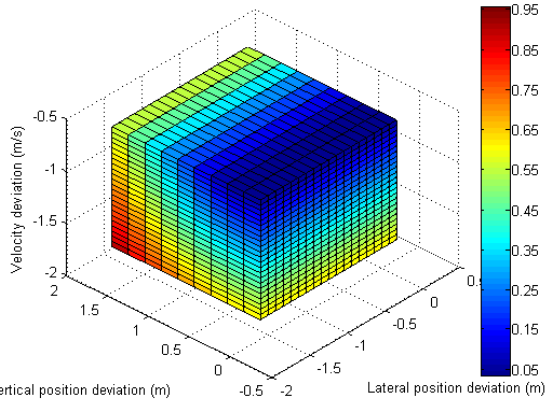

FIGURE 7. Velocity risk with lateral and vertical position deviations.

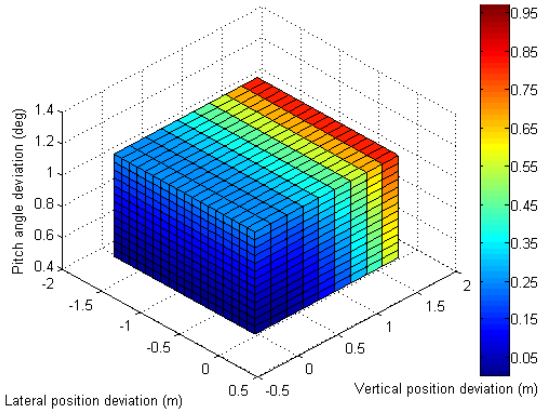

FIGURE 8. Pitch angle risk with lateral and vertical position deviations.

is constituted by current landing states, the future condition of landing risk is considered due to the subjective perception of pilots. In addition, the fuzzy logic decision from the pilots can provide nonlinear landing risk based on subjective perception. This paper defines the compensating state of the landing risk x_f, mapped from corresponding landing risk value. x_f is defined as follows:

$$x_f = W_{land} x = \begin{bmatrix} W_V 0 & 0 & 0 & -(W_{V_z}/\sin\lambda)V_z & \\ 0 & W_\phi & 0 & 0 & 0 \\ 0 & 0 & W_\theta & 0 & 0 \\ 0 & 0 & 0 & W_{V_y} & 0 \\ -(\sin\gamma)W_V V & 0 & 0 & 0 & W_{V_z} \end{bmatrix} \begin{bmatrix} V \\ \phi \\ \theta \\ V_y \\ V_z \end{bmatrix} \tag{10}$$

where, W_{land} is the landing risk about corresponding landing state, comprised by W_V, W_ϕ, W_θ, W_{V_y}, and W_{V_z}. Noted that off-diagonal nonzero elements of matrix W_{land} associated with V and V_z are due to $V_z = V \sin\gamma$. x_f will be introduced into the following NDI control structure.

Remark 2: The high-dimension landing risk model is established based on the subjective perception of the pilot behavior model. The real-time landing risk is supplied by the landing risk model for the ACLS control loops.

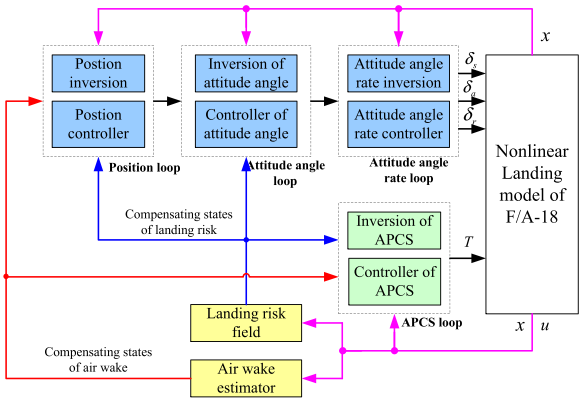

FIGURE 9. The control structure of this paper.

V. AN INNOVIATION NDI WITH COMPENSATING STATES

In this paper, there are four control loops, which are approach power compensate system (APCS) loop, position loop, attitude angle loop, and attitude angle rate loop. The APCS loop controls the approach velocity, and other loops integrated control the position and attitude of the aircraft. The control structure figure of this paper is shown below.

The loops above all include the corresponding dynamic inversions and controllers. The inversions are comprised by the landing states on the longitudinal and lateral planes, and all loops integrated consider the longitudinal and lateral coupling. Meanwhile, the reference model estimates the air wake disturbance, and the compensating states of air wake are introduced into the position loop and APCS loop. The high-dimension landing risk field calculates the landing risk in real time, and the compensating states of landing risk are introduced into the position loop, attitude angle loop, and APCS loop. All the loops not only introduce the nonlinear inversions of all directions, but also consider landing risk and air wake disturbance. Therefore, the control thought of this paper is more effective than some previous literatures. The controller structure and control parameters of each loop are independently designed, and the stable inner loop is the foundation of the outer loop.

A. CONTROL OF APCS LOOP

APCS is the basic control system in ACLS, and maintains the nearly constant approach velocity for the aircraft during landing. The approach velocity is the feedback state of APCS in this paper. In the previous references, most of APCS control laws are only comprised by the longitudinal states without considering the lateral states. However, the roll angle may decrease the approach velocity, and even results in the instability of AOA. If this phenomenon happens under the condition of short approach distance, there are fewer possibilities to wave off for the aircraft. This paper designs a nonlinear inversion, which comprehensively considers the coupling of the longitudinal and lateral landing states and introduces the compensating state of landing risk. According to Eq. (1), the thrust can be represented as follows:

$$T = \frac{m}{\cos\alpha\cos\beta}\left(\frac{1}{m}(D\cos\beta - Y\sin\beta) + g(\cos\phi\cos\theta\sin\alpha\cos\beta + \sin\phi\cos\theta\sin\beta - \sin\theta\cos\alpha\cos\beta) + \dot{V}\right) \tag{11}$$

This paper defines ΔV, as follows:

$$\Delta V = V_{cmd} - V - V_f - V_{xair} \tag{12}$$

where, V_{cmd} is the command of approach velocity, V_f is a compensating state about approach velocity from landing risk field. V_{xair} is the longitudinal component of air wake, which is introduced into the APCS loop as the compensating state about velocity from air wake estimator. An auxiliary control R_V is introduced in this paper, which is the control outputs of a PID controller for the signal ΔV. The function of R_V is to eliminate ΔV, and the control law of APCS is below:

$$T = \frac{m}{\cos\alpha\cos\beta}\left(\frac{1}{m}(D\cos\beta - Y\sin\beta) + g(\cos\phi\cos\theta\sin\alpha\cos\beta + \sin\phi\cos\theta\sin\beta - \sin\theta\cos\alpha\cos\beta) + R_V - \dot{V}_f - \dot{V}_{xair}\right) \tag{13}$$

The thrust description is a nonlinear equation, including several landing states in the longitudinal and lateral directions. In order to control the thrust by R_V, this paper defines the inversion of APCS, and introduces it into the control structure to eliminate the nonlinear factors. The diagram of control principle for APCS is as follows.

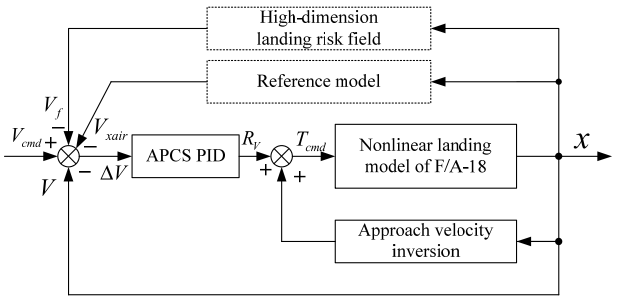

FIGURE 10. Diagram of control principle for APCS.

In Fig. 10, the approach velocity inversion is from Eq. (13). Meanwhile, the compensating state of current landing risk is introduced into the control structure, so that APCS could reduce the landing risk caused by the velocity.

B. CONTROL OF ATTITUDE ANGLE RATE LOOP

According to Eqs. (2) and (4), the attitude angle rates can be represented by the following equations:

$$\begin{bmatrix}\dot{p}\\ \dot{q}\\ \dot{r}\end{bmatrix} = \begin{bmatrix}I_{zz}/k & 0 & I_{xz}/k\\ 0 & 1/I_{yy} & 0\\ I_{xz}/k & 0 & I_{xx}/k\end{bmatrix}\left(\begin{bmatrix}M_r\\ M_t\\ M_n\end{bmatrix} - \begin{bmatrix}0 & -r & q\\ r & 0 & -p\\ -q & p & 0\end{bmatrix}\begin{bmatrix}I_{xx} & 0 & -I_{xz}\\ 0 & I_{yy} & 0\\ -I_{xz} & 0 & I_{zz}\end{bmatrix}\begin{bmatrix}p\\ q\\ r\end{bmatrix}\right) \tag{14}$$

$$\begin{bmatrix} M_r \\ M_t \\ M_h \end{bmatrix} = M(\alpha, \beta, p, q, r, V) \begin{bmatrix} \delta_s \\ \delta_a \\ \delta_r \end{bmatrix} + N(\alpha, \beta, p, q, r, V) \tag{15}$$

where, $M(\alpha, \beta, p, q, r, V)$ and $N(\alpha, \beta, p, q, r, V)$ are the polynomials of the corresponding landing states, and they are both invertible matrices. For the simply, $M(\alpha, \beta, p, q, r, V)$ and $N(\alpha, \beta, p, q, r, V)$ are represented by M and N below.

The commands of attitude angle rate are p_{cmd}, q_{cmd} and r_{cmd}. Meanwhile, Δp, Δq and Δr are the differences between the attitude angle rate and corresponding commands. The following equation is satisfied.

$$\begin{bmatrix} \Delta p \\ \Delta q \\ \Delta r \end{bmatrix} = \begin{bmatrix} p_{cmd} - p \\ q_{cmd} - q \\ r_{cmd} - r \end{bmatrix} \tag{16}$$

The auxiliary controls are defined as R_p, R_q and R_r in this paper, and they are the control outputs of three PID controllers for the signals Δp, Δq and Δr. Therefore, δ_s, δ_a and δ_r can be represented by the following equation:

$$\begin{bmatrix} \delta_s \\ \delta_a \\ \delta_r \end{bmatrix} = M^{-1} \begin{bmatrix} M_r \\ M_t \\ M_n \end{bmatrix} - N + \begin{bmatrix} R_p \\ R_q \\ R_r \end{bmatrix} \tag{17}$$

As shown by Eq. (17), the description of δ_s, δ_a and δ_r is comprised with all the landing states. This paper designs dynamic inversions of roll rate, pitch rate, and yaw rate, and the diagram of control principle for attitude angle rates is shown below.

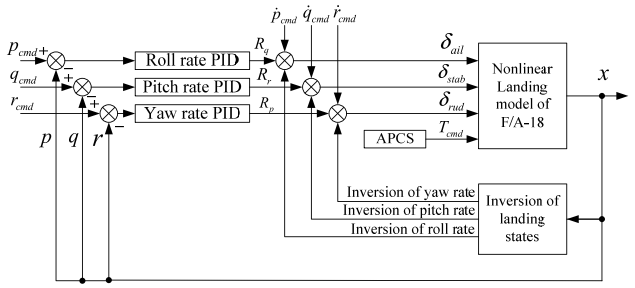

FIGURE 11. Diagram of control principle for attitude angle rates.

In Fig. 11, the dynamic inversion of the landing states is from Eq. (17), which includes the longitudinal and lateral landing states, and the controller of R_p, R_q and R_r is separately designed. Therefore, coupling of longitudinal and lateral are integrated considered so that the control accuracy can be guaranteed and the system robust is increased at the same time.

C. CONTROL OF ATTITUDE ANGLE LOOP

The attitude angles of the F/A−18 during include pitch, yaw and roll angles. However, the sideslip angle is an important variable in the lateral loop, which needs to be directly concerned and controlled. Therefore, the sideslip angle is considered in the control loop of attitude angles in this paper. Considering the special feather of yaw angle in the lateral loop, this paper will detailed described the control of yaw angle in the next section, and the NDI structure of the attitude angles include roll, pitch, and sideslip angles. The attitude angles could be described:

$$\begin{cases} \begin{bmatrix} \dot{\phi} \\ \dot{\theta} \\ \dot{\beta} \end{bmatrix} = \begin{bmatrix} 1 & \sin\phi\tan\theta & \cos\phi\tan\theta \\ 0 & \cos\phi & -\sin\phi \\ \sin\alpha & 0 & -\cos\alpha \end{bmatrix} \begin{bmatrix} p \\ q \\ r \end{bmatrix} + \begin{bmatrix} 0 \\ 0 \\ P \end{bmatrix} \\ P = \dfrac{1}{mV}(Y\cos\beta + D\sin\beta) + \dfrac{g}{V}\cos\beta\sin\phi\cos\theta \\ \quad + \dfrac{\sin\beta}{V}(g\cos\alpha\sin\theta - g\sin\alpha\cos\phi\cos\theta + \dfrac{T}{m}\cos\alpha) \end{cases} \tag{18}$$

The commands of attitude angle are ϕ_{cmd}, θ_{cmd}, and β_{cmd}. Meanwhile, $\Delta\phi$, $\Delta\theta$, and $\Delta\beta$ are the differences between the attitude angle and corresponding commands. The following equation is satisfied.

$$\begin{bmatrix} \Delta\phi \\ \Delta\theta \\ \Delta\beta \end{bmatrix} = \begin{bmatrix} \phi_{cmd} - \phi - \phi_f \\ \theta_{cmd} - \theta - \theta_f \\ \beta_{cmd} - \beta \end{bmatrix} \tag{19}$$

where, ϕ_f and θ_f are the compensating state about roll and pitch angles from the landing risk field.

The auxiliary controls for the attitude angles are defined as R_ϕ, R_θ, and R_β in this paper, and they are the control outputs of three PID controller for $\Delta\phi$, $\Delta\theta$, and $\Delta\beta$. Therefore, p_{cmd}, q_{cmd}, and r_{cmd} can be represented:

$$\begin{bmatrix} p_{cmd} \\ q_{cmd} \\ r_{cmd} \end{bmatrix} = \begin{bmatrix} 1 & \sin\phi\tan\theta & \cos\phi\tan\theta \\ 0 & \cos\phi & -\sin\phi \\ \sin\alpha & 0 & -\cos\alpha \end{bmatrix}^{-1} \times \left(\begin{bmatrix} R_\phi \\ R_\theta \\ R_\beta \end{bmatrix} - \begin{bmatrix} 0 \\ 0 \\ P \end{bmatrix} \right) \tag{20}$$

The control principle for attitude angles is shown below.

The control structure of attitude angles proposed by this paper is different from the previous literatures: (1) The sideslip angle is introduced into the control targets so that it can be directly controlled; (2) The compensating states about ϕ and θ from the landing risk field is introduced into the control targets so that the state deviations and landing risk are both eliminated.

D. CONTROL OF POSITION LOOP

The vertical position and lateral position are controlled through changing pitch angle and roll angle, respectively. However, if the yaw angle is not considered, the lateral position of the aircraft is likely out of control due to sudden changes of the side force of the aircraft. Hence, the yaw angle in the process of lateral position loop is introduced in this paper, so that the stability of lateral loop can be maintained. According to Eq. (3), the following equation is satisfied:

$$\dot{\psi} = q\sec\theta\sin\phi + r\sec\theta\cos\phi \tag{21}$$

The equation above is linearized under the condition of ϕ_t, so $\dot{\psi}$ could be represented by the following:

$$\dot{\psi} = q\sec\theta\sin\phi_t + r\sec\theta\cos\phi_t + (q\sec\theta\cos\phi_t - r\sec\theta\sin\phi_t)(\phi - \phi_t) \quad (22)$$

This paper defines the auxiliary control about the attitude angles R_ψ, and the command of roll angle $\phi_{cmd}$is:

$$\phi_{cmd} = \frac{R_\psi - (q\sec\theta\sin\phi_t + r\sec\theta\cos\phi_t)}{(q\sec\theta\cos\phi_t - r\sec\theta\sin\phi_t)} + \phi_t \quad (23)$$

According to the equation above, the changing rates of aircraft position in the vertical and lateral directions in the ground coordinate system $\dot{P}_{yg}$ and $\dot{P}_{zg}$ can be described as:

$$\begin{cases} \dot{P}_{yg} = F(\psi) = (V\cos\theta\cos\beta\cos\alpha + V\sin\phi\sin\theta\sin\beta \\ \quad + V\cos\phi\sin\theta\cos\beta\sin\alpha)\sin\psi + (V\cos\phi\sin\beta \\ \quad - V\sin\phi\cos\beta\sin\alpha)\cos\psi \\ \dot{P}_{zg} = G(\theta) = -V\cos\beta\cos\alpha\sin\theta + (V\sin\phi\sin\beta \\ \quad + V\cos\phi\cos\beta\sin\alpha)\cos\theta \end{cases} \quad (24)$$

It is assumed that the equilibrium roll and pitch angles are ψ_t and θ_t, and the roll and pitch angles could be described by equilibrium and difference of them, as follows:

$$\begin{cases} \psi = \psi_t + \Delta\psi \\ \theta = \theta_t + \Delta\theta \end{cases} \quad (25)$$

Given to Eq. (25), Eq. (24) could be rewritten as follows:

$$\begin{cases} \dot{P}_{yg} = (V\cos\theta\cos\beta\cos\alpha + V\sin\phi\sin\theta\sin\beta \\ \quad + V\cos\phi\sin\theta\cos\beta\sin\alpha)\sin(\psi_t + \Delta\psi) \\ \quad + (V\cos\phi\sin\beta - V\sin\phi\cos\beta\sin\alpha)\cos(\psi_t + \Delta\psi) \\ \dot{P}_{zg} = -V\cos\beta\cos\alpha\sin(\theta_t + \Delta\theta) + (V\sin\phi\sin\beta \\ \quad + V\cos\phi\cos\beta\sin\alpha)\cos(\theta_t + \Delta\theta) \end{cases} \quad (26)$$

$\dot{P}_{yg}$ and $\dot{P}_{yg}$ could be linearized under the condition of ψ_t and θ_t, and the following equations are satisfied:

$$\begin{cases} \dot{P}_{yg} = F(\psi_t) + \left.\dfrac{\partial F}{\partial\psi}\right|_{\psi=\psi_t} (\psi - \psi_t) \\ \dot{P}_{zg} = G(\theta_t) + \left.\dfrac{\partial G}{\partial\theta}\right|_{\theta=\theta_t} (\theta - \theta_t) \end{cases} \quad (27)$$

The position deviations of the aircraft in the lateral and vertical directions are described as ΔP_{yg} and ΔP_{zg}:

$$\begin{bmatrix} \Delta P_{yg} \\ \Delta P_{zg} \end{bmatrix} = \begin{bmatrix} P_{yg\_cmd} - P_{yg} - \int_0^t V_{yf}(\tau)d\tau - \int_0^t V_{yair}(\tau)d\tau \\ P_{zg\_cmd} - P_{zg} - \int_0^t V_{zf}(\tau)d\tau - \int_0^t V_{zair}(\tau)d\tau \end{bmatrix} \quad (28)$$

The auxiliary control for the aircraft positions are defined as R_{P_y} and R_{P_z} in this paper, which means the control outputs of two PID controller for ΔP_{yg} and ΔP_{zg}. The commands of yaw angle ψ_{cmd} and pitch angle θ_{cmd} are:

$$\begin{cases} \psi_{cmd} = \psi_t + \dfrac{R_{P_y} - H_1(\psi_t)}{H_2(\psi_t)} \\ \theta_{cmd} = \theta_t - \dfrac{R_{P_z} + J_1(\theta_t)}{J_2(\theta_t)} \end{cases} \quad (29)$$

$$\begin{cases} H_1(\psi_t) = (V\cos\theta\cos\beta\cos\alpha + V\sin\phi\sin\theta\sin\beta \\ \quad + V\cos\phi\sin\theta\cos\beta\sin\alpha)\sin\psi_t \\ \quad + (V\cos\phi\sin\beta - V\sin\phi\cos\beta\sin\alpha)\cos\psi_t \\ H_2(\psi_t) = (V\cos\theta\cos\beta\cos\alpha + V\sin\phi\sin\theta\sin\beta \\ \quad + V\cos\phi\sin\theta\cos\beta\sin\alpha)\cos\psi_t \\ \quad - (V\cos\phi\sin\beta - V\sin\phi\cos\beta\sin\alpha)\sin\psi_t \\ J_1(\theta_t) = V\cos\beta\cos\alpha\sin\theta_t \\ \quad - (V\sin\phi\sin\beta + V\cos\phi\cos\beta\sin\alpha)\cos\theta_t \\ J_2(\theta_t) = V\cos\beta\cos\alpha\cos\theta_t \\ \quad + (V\sin\phi\sin\beta + V\cos\phi\cos\beta\sin\alpha)\sin\theta_t \end{cases} \quad (30)$$

The diagram of control principle for positions is below.

The dynamic inversions of vertical and lateral positions are comprised by the complex landing states in both directions. The compensating states from the landing risk field and reference model are introduced into the command signals. The positions of the aircraft are determined by the landing state deviations, integrated with landing risk and air wake, so the landing safety is increased by this paper.

Remark 3: The compensating states of the air wake components and landing risk are introduced into the APCS loop, attitude angle rate loop, attitude angle loop, and position loop of ACLS control law. Therefore, the landing state deviations, air wake disturbance, and landing risk can be eliminated in the rolling optimization process.

VI. ANALYSIS OF STABILITY OF ACLS

The PID with appropriate parameters could maintain system stability, which is proved by many references and practical applications. There are several control loops in this paper, and APCS loop is taken for instance here. According to the APCS control signals, there is the following equation:

$$\begin{cases} \Delta\dot{V} = -R_V \\ \Delta V = V_{cmd} - V - V_f - V_{xair} \end{cases} \quad (31)$$

The control strategy proposed by this paper is:

$$R_V = K_P\Delta V + K_I\int_0^t \Delta V d\tau + K_D\Delta V/\Delta t \quad (32)$$

Eq. (32) is substituted into Eq. (31), and $\Delta V$is satisfied:

$$\Delta\ddot{V} + K_P\Delta\dot{V} + K_I\Delta V = 0 \quad (33)$$

The equation above is an exponential stable error system. When the initial approach velocity deviation satisfies $\Delta V(0) = \Delta\dot{V}(0) = 0$, then $\Delta V(t) \equiv 0, \forall t > 0$. Therefore, the NDI control system of APCS could track the desired approach velocity. Otherwise, $\Delta V(t)$ converges to 0 within

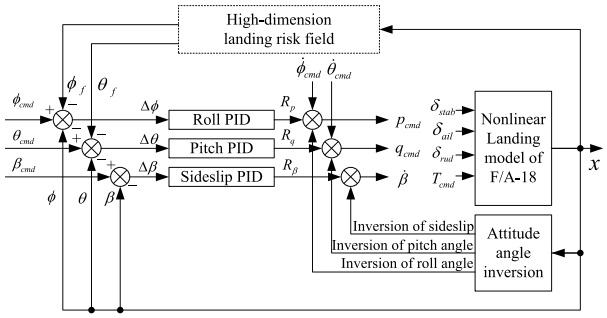

FIGURE 12. Diagram of control principle for attitude angles.

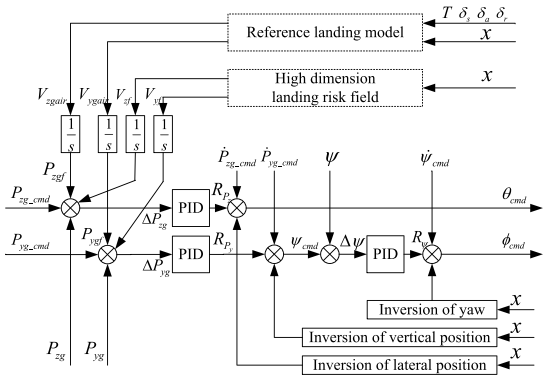

FIGURE 13. Diagram of control principle for aircraft positions.

FIGURE 14. A semi-physical landing simulator.

exponential rate. Other NDI loops are similar as the APCS loop, which is not described here due to the space limitation.

VII. NUMERICAL SIMULATION RESULTS

The verification of the proposed algorithm by this paper is completed on a semi-physical simulator, as shown by Fig. 14. The nonlinear landing model, the reference model, and the NDI control law are realized by Matlab software. The three-dimensional scene and evaluation analysis modules of the landing process are realized by Vega Prime 6.0 and Visual Studio 2010. The network communication is introduced to finish data interactions of simulator and other modules.

This paper completes three cases of simulations, i.e., one is the proposed method by this paper, and the second one is not

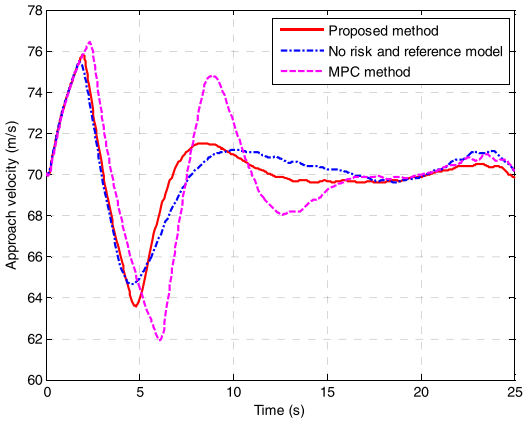

FIGURE 15. Approach velocity curves.

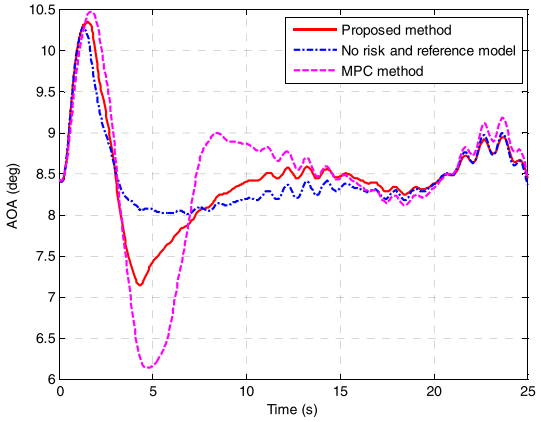

FIGURE 16. AOA curves.

considering the landing risk factors and air wake disturbance, and the third one is model predictive control considering subjective landing risk from [19]. For an accurate comparison, the same control parameters of the first two simulations are acquired, and the weights of state and control terms in the third method are adjusted to satisfy the initial conditions. The simulating curves are marked by "The proposed method", "No risk and reference model", and "MPC method", respectively. The initial vertical and lateral deviations are respective 15 m and 5 m, and initial values of other states are the equilibrium values. The comparing curves in the simulations are shown below.

Figs. 15−16 show the comparison curves of the approach velocity and the AOA. First of all, the velocity and AOA of the proposed method reach the desired values more quickly than the compared methods. Second, the overshoot of the proposed method after steady states is less than that of the compared methods. In addition, the effect of eliminating air wake through the proposed method is slightly better than the compared methods due to the compensating states of the reference model. The MPC method is weak in reducing disturbance. In Fig. 17, the sideslip angle curve of the proposed method is less than the compared methods after 4 seconds,

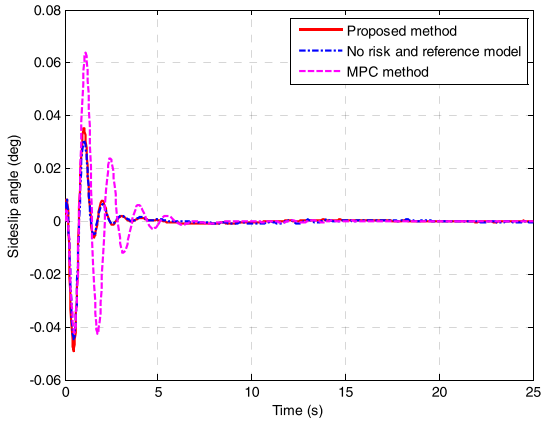

FIGURE 17. Sideslip angle curves.

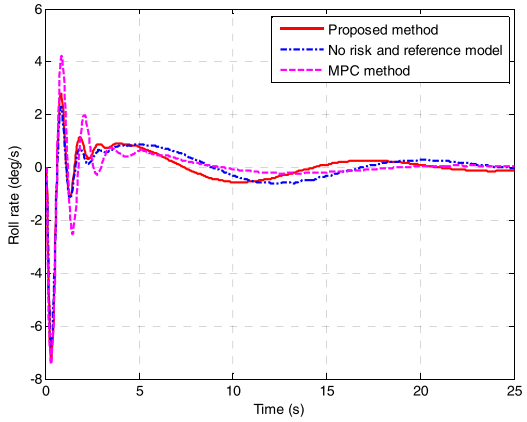

FIGURE 18. Roll rate curves.

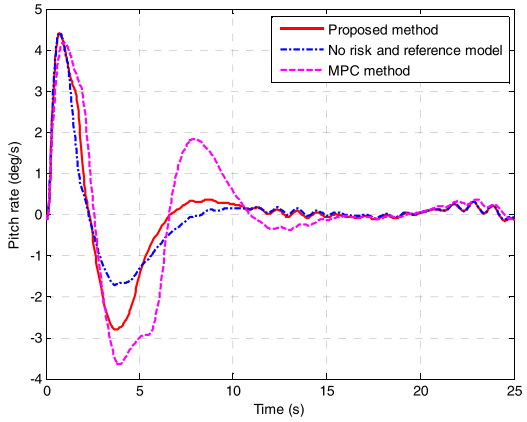

FIGURE 19. Pitch rate curves.

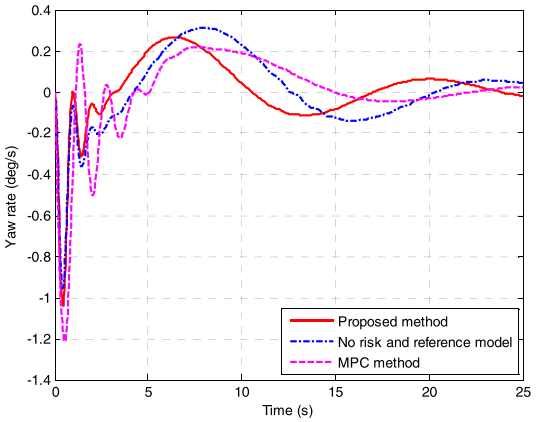

FIGURE 20. Yaw rate curves.

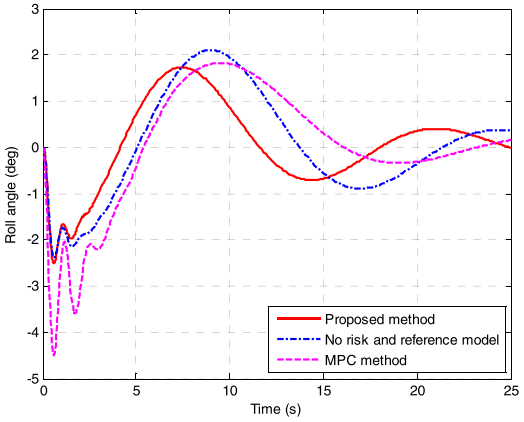

FIGURE 21. Roll angle curves.

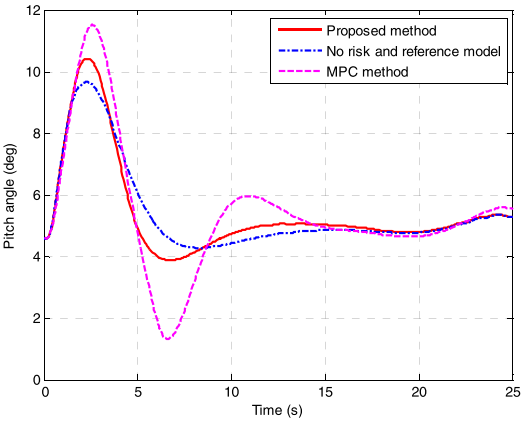

FIGURE 22. Pitch angle curves.

which is caused by the introduction of the sideslip angle in the NDI loop of attitude angle. Especially, the sideslip angle of MPC method is greater than the proposed method.

The comparison curves of the attitude angle rates are described by Figs. 18−20. The rapidity of the roll rate, pitch rate and yaw rate through the proposed method is a little more optimal than the second method, and much more optimal than the MPC method. The more rapid attitude angle rates are controlled, the more excellent effect control augmentation system performs. Therefore, the deviations of the roll angle, pitch angle, and yaw angle are more quickly reduced by the proposed method than the compared methods, as shown by Figs. 21−23. Especially, the overshoots of the pitch and yaw angles by MPC method is greater than other methods. Therefore, the consideration of the compensating states of landing risk is more effective than the compared method.

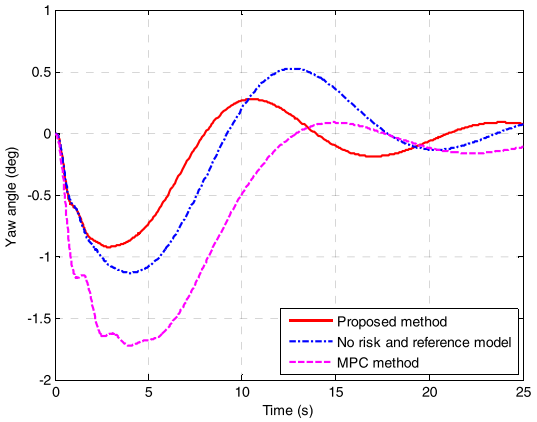

FIGURE 23. Yaw angle curves.

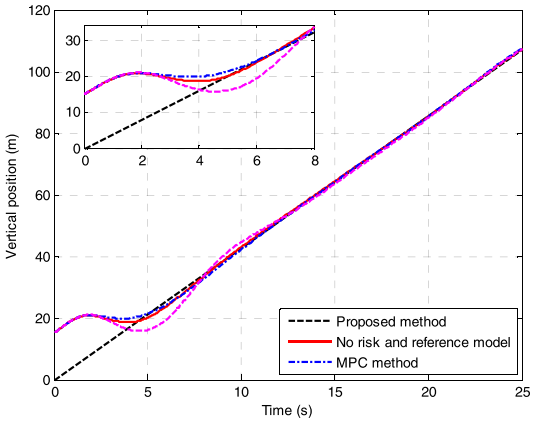

FIGURE 25. Desired and actual vertical position curves.

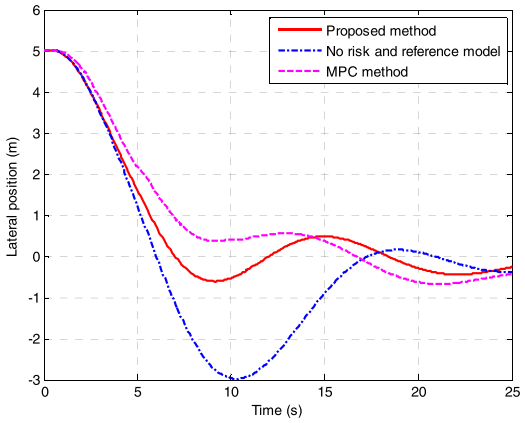

FIGURE 24. Lateral position curves.

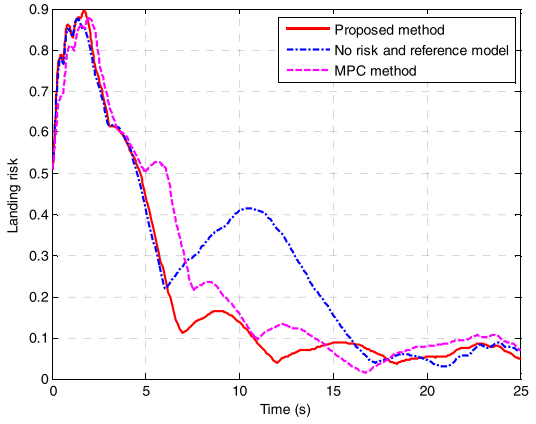

FIGURE 26. Landing risk curves.

Figs. 24−25 show the lateral and vertical positions. The proposed method eliminates the vertical deviation faster than that of the compared methods, and the vertical deviation by MPC method is greatest in these three methods. Furthermore, the lateral position overshoot of the proposed method is much less than the compared methods. There are two reason of this phenomenon. First of all, the control of yaw angle is included in the lateral position loop. Second, the compensating states of the air wake and landing risk are introduced into the position loops. It looks like that the lateral deviation curve is more smooth and steady than that of the proposed method, but the MPC method does not eliminate the lateral deviation in time so that the effect of MPC method is not good. Therefore, the method investigated by this paper could control the aircraft position more effectively and safely. Fig. 26 shows the landing risk curves. Due to the same initial condition, the landing risks of the first 5 seconds in these three methods are nearly same. However, the proposed method introduces the compensating states of the high-dimension risk field so that the landing risk is eliminated step by step. By contrast, the landing risk of MPC method and another compared method is abnormally high from 5 s to 8 s and 6 s to 15 s, respectively. This condition is very dangerous for the aircraft safety. Furthermore, the simulated landing time is 25 s, which is based on the glide slope length and aircraft velocity. The actual time is about 10 s. Therefore, the algorithm proposed by this paper can simulate landing process in real time.

Remark 4: The proposed method, a NDI method without considering the landing risk and air wake, and a MPC method considering the subjective landing risk are simulated and compared in this paper. The robustness, the ability of eliminating air wake disturbance and landing risk, and rapidity of control system are improved significantly by the proposed method. The control effect of this paper is more effective than some previous literatures.

VIII. CONCLUSION

This paper constructs an ACLS control law, utilizing an innovative NDI control method with the compensating states. The control law integrated considers the coupling of the longitudinal and lateral loops, the landing risk, and the air wake disturbance. This paper proposes a high-dimension field of the landing risk and a reference model to calculate the compensation states, which are introduced into the control structure to improve the control effects. From the comparison in the simulations, the following conclusions are acquired:

(1) The landing mission could be completed through the proposed method, and the performances of the longitudinal and lateral loops are all excellent. The simulation curves prove that the proposed method solves the complicated coupling problem.
(2) Based on the experiences of the pilots, the landing risk field considers multi-landing states and fully reflects the current and future landing danger factors.
(3) The introduction of the compensating states from the high-dimension landing risk field and the reference model, increase the rapidity and robustness of the control system. According to simulated step, the whole simulated landing time, and actual time spent by the computer, the landing risk and air wake disturbance can be reduced in real-time, and the algorithm of this paper can realize the control in real-time.. Furthermore, the landing state deviations, landing risk, and the air wake disturbance are eliminated more obviously than the previous reference.

Through the simulated comparison, the method proposed by this paper can actively eliminate disturbances due to compensate the corresponding states, and decrease the nonlinearity effects based on the NDI method. This paper considers some mainly complex influences of landing process, and realizes the precise control target.

This paper does not considering the deck motion compensation, which will be researched in the future work.

REFERENCES

[1] "Human factors in fatal aircraft accidents," Dept. Transp. Regional Develop., Bureau Air Saf. Invest., Canberra, ACT, Australia, Tech. Rep., 1996.
[2] Y. Dai, J. Tian, H. Rong, and T. D. Zhao, "Hybrid safety analysis method based on SVM and RST: An application to carrier landing of aircraft," *Saf. Sci.*, vol. 80, pp. 56–65, Dec. 2015. doi: 10.1016/j.ssci.2015.07.006.
[3] L. Wang, Q. Zhu, Z. Zhang, and R. Dong, "Modeling pilot behaviors based on discrete-time series during carrier-based aircraft landing," *J. Aircr.*, vol. 53, no. 6, pp. 1922–1931 Nov. 2016. doi: 10.2514/1.C033721.
[4] T. Rudowsky *et al.*, "Review of the carrier approach criteria for carrier-based aircraft," Nav. Air Warfare Center Aircr. Division, Patuxent River, MD, USA, Tech. Rep. NAWCADPAX/TR-2002/71, 2002.
[5] J. M. Urnes and R. K. Hess, "Development of the F/A-18A automatic carrier landing system," *J. Guid.*, vol. 8, no. 3, pp. 289–295, May 1985. doi: 10.2514/3.19978.
[6] J. M. Urnes, R. K. Hess, and R. F. Moomaw, "Development of the navy H-dot automatic carrier landing system designed to give improved approach control in air turbulence," in *Proc. AIAA Guid. Control Conf.*, Washington, DC, USA, Aug. 1979, pp. 491–501. doi: 10.2514/6.1979-1772.
[7] L. M. Yue, G. Liu, and G. X. Hong, "Design and simulation of F/A-18A automatic carrier landing guidance controller," in *Proc. AIAA Modeling Simulation Technol. Conf.*, Washington, DC, USA, Jun. 2016, pp. 1–11. doi: 10.2514/6.2016-3527.
[8] R. Lungu and M. Lungu, "Automatic landing control using H-inf control and dynamic inversion," *Proc. Inst. Mech. Eng., G, J. Aerosp. Eng.*, vol. 228, no. 14, pp. 2612–2626, Dec. 2014. doi: 10.1177/0954410014523576.
[9] R. Lungu and M. Lungu, "Design of automatic landing systems using the H-inf control and the dynamic inversion," *J. Dyn. Sys., Meas., Control*, vol. 138, no. 2, Feb. 2016, Art. no. 024501. doi: 10.1115/1.4032028.
[10] R. Lungu and M. Lungu, "Automatic landing system using neural networks and radio-technical subsystems," *Dec. J. Aeronaut.*, vol. 30, no. 1, pp. 399–411, Feb. 2017. doi: 10.1016/j.cja.2016.12.019.
[11] M. Lungu and R. Lungu, "Automatic control of aircraft lateral-directional motion during landing using neural networks and radio-technical subsystems," *Neurocomputing*, vol. 171, pp. 471–481, Jan. 2016. doi: 10.1002/asjc.1133.
[12] D. M. K. K. V. Rao and T. H. Go, "Automatic landing system design using sliding mode control," *Aerosp. Sci. Technol.*, vol. 32, no. 1, pp. 180–187, Jan. 2014. doi: 10.1016/j.ast.2013.10.001.
[13] F. Zheng, Z. Zhen, and H. Gong, "Observer-based backstepping longitudinal control for carrier-based UAV with actuator faults," *J. Syst. Eng. Electron.*, vol. 28, no. 2, pp. 322–337, Apr. 2017. doi: 10.21629/JSEE.2017.02.14.
[14] Z. Guan, Y. Ma, Z. Zheng, and N. Guo, "Prescribed performance control for automatic carrier landing with disturbance," *Nonlinear Dyn.*, vol. 94, no. 2, pp. 1335–1349, Oct. 2018. doi: 10.1007/s11071-018-4427-3.
[15] K. Subbarao and M. Ahmed, "Nonlinear guidance and control laws for three-dimensional target tracking applied to unmanned aerial vehicles," *J. Aerosp. Eng.*, vol. 27, no. 3, pp. 604–610, May 2014. doi: 10.1061/(ASCE)AS.1943-5525.0000275.
[16] Z. Zhen, S. Jiang, and J. Jiang, "Preview control and particle filtering for automatic carrier landing," *IEEE Trans. Aerosp. Electron. Syst.*, vol. 54, no. 6, pp. 2662–2674, Dec. 2018. doi: 10.1109/TAES.2018.2826398.
[17] H. Q. Wang, P. X. Liu, and B. Niu, "Robust fuzzy adaptive tracking control for nonaffine stochastic nonlinear switching systems," *IEEE Trans. Cybern.*, vol. 48, no. 8, pp. 2462–2471, Aug. 2018. doi: 10.1109/TCYB.2017.2740841.
[18] H. Wang, H. Karimi, P. X. Liu, and H. Yang, "Adaptive neural control of nonlinear systems with unknown control directions and input dead-zone," *IEEE Trans. Syst., Man, Cybern. Syst.*, vol. 48, no. 11, pp. 1897–1907, Nov. 2018. doi: 10.1109/TSMC.2017.2709813.
[19] L. P. Wang, Z. Zhang, Q. D. Zhu, and R. Dong, "Longitudinal automatic carrier landing system guidance law using model predictive control with an additional landing risk term," *Proc. Inst. Mech. Eng., G, J. Aerosp. Eng.*, vol. 233, no. 3, pp. 1089–1105, Mar. 2017. doi: 10.1177/0954410017746432.
[20] T. Woodbury and J. Valasek, "Synthesis and flight test of automatic landing controller using quantitative feedback theory," *J. Guid. Control Dyn.*, vol. 39, no. 9, pp. 1994–2010 Sep. 2016. doi: 10.2514/1.G001758.
[21] J. N. Li and H. B. Duan, "Simplified brain storm optimization approach to control parameter optimization in F/A-18 automatic carrier landing system," *Aerosp. Sci. Technol.*, vol. 42, pp. 187–195 Apr./May 2015. doi: 10.1016/j.ast.2015.01.017.
[22] R. Dou and H. Duan, "Lévy flight based pigeon-inspired optimization for control parameters optimization in automatic carrier landing system," *Aerosp. Sci. Technol.*, vol. 61, pp. 11–20, Feb. 2017. doi: 10.1016/j.ast.2016.11.012.
[23] R. Lungu and M. Lungu, "Automatic control of aircraft in lateral-directional plane during landing," *Asian J. Control*, vol. 18, no. 2, pp. 433–446, Mar. 2016. doi: 10.1002/asjc.1133.
[24] M. Brodecki and K. Subbarao, "Autonomous formation flight control system using in-flight sweet-spot estimation," *J. Guid. Control Dyn.*, vol. 38, no. 6, pp. 1083–1096, Jun. 2015. doi: 10.2514/1.G000220.
[25] H. Bouadi, F. Mora-Camino, and D. Choukroun, "Space-indexed control for aircraft vertical guidance with time constraint," *J. Guid. Control Dyn*, vol. 37, no. 4, pp. 1103–1113, Jul. 2014. doi: 10.2514/1.62118.
[26] P. K. Menon, S. S. Vaddi, and P. Sengupta, "Robust landing guidance law for impaired aircraft," *J. Guid. Control Dyn.*, vol. 35, no. 6, pp. 1865–1877, Nov. 2012. doi: 10.2514/1.54213.
[27] C. E. Lan and R. C. Chang, "Unsteady aerodynamic effects in landing operation of transport aircraft and controllability with fuzzy-logic dynamic inversion," *Aerosp. Sci. Technol.*, vol. 78, pp. 354–363, Jul. 2018. doi: 10.1016/j.ast.2018.04.032.
[28] X. Zhao, H. Yang, W. Xia, and X. Wang, "Adaptive fuzzy hierarchical sliding-mode control for a class of MIMO nonlinear time-delay systems with input saturation," *IEEE Trans. Fuzzy Syst.*, vol. 25, no. 5, pp. 1062–1077, Oct. 2017. doi: 10.1109/TFUZZ.2016.2594273.
[29] X. Zhao, X. Zheng, B. Niu, and L. Liu, "Adaptive tracking control for a class of uncertain switched nonlinear systems," *Automatica*, vol. 52, pp. 185–191, Feb. 2015. doi: 10.1016/j.automatica.2014.11.019.
[30] I. Hameduddin and A. H. Bajodah, "Nonlinear generalised dynamic inversion for aircraft manoeuvring control," *Int. J. Control*, vol. 85, no. 4, pp. 437–450, Feb. 2012. doi: 10.1080/00207179.2012.656143.
[31] J. T. Luxhøj, "A conceptual object-oriented Bayesian network (OOBN) for modeling aircraft carrier-based UAS safety risk," *J. Risk Res*, vol. 18, no. 10, pp. 1230–1258, Nov. 2015. doi: 10.1080/13669877.2014.913664.

[32] J. Tian and Y. Dai, "Research on the relationship between mishap risk and time margin for control: A case study for carrier landing of aircraft," *Cognition, Technol. Work*, vol. 10, no. 16, pp. 259–270, May 2014. doi: 10.1007/s10111-013-0262-y.
[33] A. Washington, R. A. Clothier, and J. Silva, "A review of unmanned aircraft system ground risk models," *Prog. Aeosp. Sci.*, vol. 95, pp. 24–44, Nov. 2017. doi: 10.1016/j.paerosci.2017.10.001.
[34] L. Wang, Y. Ren, and C. X. Wu, "Effects of flare operation on landing safety: A study based on ANOVA of real flight data," *Saf. Sci.*, vol. 102, pp. 14–25, Feb. 2018. doi: 10.1016/j.ssci.2017.09.027.
[35] L. N. Aleksandrovskyaa, A. E. Ardalionova, and A. V. Kirillin, "Ultra-low risk assessment under the confirmed compliance of automatic aircraft landing characteristics with airworthiness requirements," *J. Comput. Syst. Sci. Int.*, vol. 55, no. 2, pp. 232–241, Mar. 2016. doi: 10.1134/S1064230716010032.
[36] Y. Lu, S. Zhang, and X. Li, "A hazard analysis-based approach to improve the landing safety of a BWB remotely piloted vehicle," *Chin. J. Aeronaut.*, vol. 25, no. 6, pp. 846–853, Dec. 2012. doi: 10.1016/S1000-9361(11)60454-8.
[37] R. M. A. Valdés, F. G. Comendador, L. M. Gordún, "The development of probabilistic models to estimate accident risk (due to runway overrun and landing undershoot) applicable to the design and construction of runway safety areas," *Saf. Sci.*, vol. 49, pp. 633–650, Jun. 2011. doi: 10.1016/j.ssci.2010.09.020.
[38] F. Schettini, G. Di Rito, E. Denti, and R. Galatolo, "Wind identification via Kalman filter for aircraft flow angles calibration," in *Proc. IEEE Int. Workshop Metrology AeroSpace (MetroAeroSpace)*, Padua, Italy, Jun. 2017, pp. 97–102.
[39] A. Wenz and T. A. Johansen, "Estimation of wind velocities and aerodynamic coefficients for UAVs using standard autopilot sensors and a moving horizon estimator," in *Proc. Int. Conf. Unmanned Aircr. Syst. (ICUAS)*, Miami, FL, USA, Jun. 2017, pp. 1267–1276.
[40] A. Chakraborty, P. Seiler, and G. J. Balas, "Applications of linear and nonlinear robustness analysis techniques to the F/A-18 flight control laws," in *Proc. AIAA Guid., Navigat., Control Conf.*, Washington, DC, USA, Aug. 2009, pp. 10–13. doi: 10.2514/6.2009-5675.
[41] A. Chakraborty, P. Seiler, and G. J. Balas, "Susceptibility of F/A-18 flight controllers to the falling-leaf mode: Nonlinear analysis," *J. Guid. Control Dyn.*, vol. 34, no. 1, pp. 57–72 Jan. 2011. doi: 10.2514/1.50675.
[42] M. B. Subrahmanyam, "H-infinity design of F/A-18A automatic carrier landing system," *J. Guid. Control Dyn.*, vol. 17, no. 1, pp. 187–191, Jan. 1994. doi: 10.2514/3.21177.
[43] B. Xu, D. Wang, Y. Zhang, and Z. Shi, "DOB-based neural control of flexible hypersonic flight vehicle considering wind effects," *IEEE Trans. Ind. Electron.*, vol. 64, no. 11, pp. 8676–8685, Nov. 2017. doi: 10.1109/TIE.2017.2703678.
[44] L. Wang and J. Su, "Robust disturbance rejection control for attitude tracking of an aircraft," *IEEE Trans. Control Syst. Technol.*, vol. 23, no. 6, pp. 2361–2368, Nov. 2015. doi: 10.1109/TCST.2015.2398811.
[45] *Flying Qualities of Pilot Aircraft*, Standards MIL-HDBK-1797, 1997.

LIPENG WANG was born in Harbin, China, in 1985. He received the B.A. degree in automatic control, the M.Sc. degree in control theory and control engineering, and the Ph.D. degree in control science and engineering from Harbin Engineering University, in 2009, 2012, and 2017, respectively, where he is currently a Lecturer with the College of Automation. His research interests include model predictive control, aerospace safety, and aerospace control.

ZHI ZHANG was born in Jiamusi, China, in 1981. He received the B.A. degree in measurement and control technology and instrument, the M.Sc. degree in control theory and control engineering, and the Ph.D. degree in control science and engineering from Harbin Engineering University in 2003, 2006, and 2007, respectively, where he is currently a Professor with the College of Automation. His research interests include aerospace control and robot vision systems.

QIDAN ZHU was born in Harbin, China, in 1963. He is currently the Chair of the Intelligent Control Laboratory, College of Automation, Harbin Engineering University. His current research interests include intelligent control and machine visions.

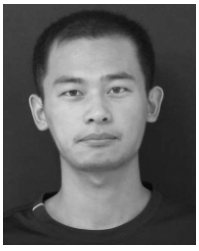

ZIXIA WEN is currently the Senior Engineer with the AVIC Xi'an Flight Automatic Control Research Institute. His research interest includes model predictive control and UAV guidance and control.